Quantitative assessment of the Effect of Anode Surface Roughness on Diagnostic X-ray Spectra: A Monte Carlo Simulation Study

A. Mehranian, *Student Member, IEEE,* M. R. Ay, *Member, IEEE*, N. Riyahi Alam and H. Zaidi, *Senior Member, IEEE*

***Abstract* – An experimental measurement study involving surface profilometry and scanning electron microscopy (SEM) combined with MCNP4C-based Monte Carlo simulations was performed to evaluate anode surface roughness in aged x-ray tubes and to quantitatively predict its impact and relevance on generated diagnostic x-ray spectra. Surface profilometry determined that the center-line average roughness in the most aged x-ray tube evaluated in our study was around 50 μm. SEM measurements also revealed valuable details about the morphology of cracks and irregularities on the anode's focal path. An image-based modeling method was followed for defining more realistic models from the surface-cracked anodes into MCNP's environment. In this approach, the matrices of focal spot images were numerically processed such that the mean depth of cracks along with their spatial pattern to be incorporated into pixel values in agreement with the measured average depths. By invoking MCNP4C's Gaussian energy broadening (GEB), the correctness of this code in simulating diagnostic x-ray spectra was well validated against experimentally-measured spectra. The simulated spectra in surface deteriorated anode models were compared with those simulated in perfectly plain anodes considered as reference. From these comparisons, an intensity loss of 4.5% and 16.8% was predicted for anodes aged by 5 and 50 μm-deep cracks in conditions of 50 kVp, 6 degree target angle, 2.5 mm Al total filtration. By deploying several point detectors (F5 tallies) along the anode-cathode direction and averaging exposure over them, it was found that for a 12 degree anode roughened by 50 µm-deep cracks, the reduction of overall exposure is 14.9% and 13.1% for 70 and 120 kVp tube voltages, respectively. Finally, change in patient entrance skin dose (ESD), as a result of anode roughness, was assessed under various conditions in a chest x-ray radiography examination. In conclusion, anode surface roughness can have a non negligible effect on output spectra in aged x-ray imaging tubes and as such, depending on x-ray tube's workload, its impact should be carefully considered in medical x-ray imaging systems.**

This work was supported by Tehran University of Medical Sciences under grant No. 8595-300188 and the Swiss National Foundation under grant No. 31003A-125246.

A. Mehranian is with the Department of Medical Physics and Biomedical Engineering, Tehran University of Medical Sciences, Tehran, Iran and Research Center for Science and Technology in Medicine, Tehran University of Medical Sciences, Tehran, Iran (e-mail: mehranian@razi.tums.ac.ir).

M. R. Ay is with the Department of Medical Physics and Biomedical Engineering, Tehran University of Medical Sciences, Tehran, Iran and Research Center for Science and Technology in Medicine, Tehran University of Medical Sciences, Iran and Research Institute for Nuclear Medicine, Tehran University of Medical Sciences, Tehran, Iran (e-mail: mohammadreza_ay@sina.tums.ac.ir).

N. Riyahi Alam is with the Department of Medical Physics and Biomedical Engineering, Tehran University of Medical Sciences, Tehran, Iran (e-mail: riahinad@sina.tums.ac.ir).

H. Zaidi is with the Division of Nuclear Medicine, Geneva University Hospital, CH-1211 Geneva, Switzerland and Geneva Neuroscience Center, Geneva University, CH-1205 Geneva, Switzerland (e-mail: habib.zaidi@hcuge.ch).

I. Introduction

Accurate knowledge of diagnostic x-ray spectra under conditions of clinical x-ray examinations and the assessment of factors influencing them has been a long-standing goal in diagnostic imaging where it was attempted to obtain high quality diagnostic images while keeping to a reasonable level patient dose. Since the experimental measurement of x-ray spectra requires considerable time and effort, there has been an increasing interest in the development of computational models to predict x-ray spectra under conditions typically encountered in clinical setting since the early 1920s. One of their advantages is that they allow to separate factors which cannot be isolated and studied in experimental settings. Hence, during the last few decades, extensive efforts have been directed towards the development of computational models taking into account the physics x-ray imaging to accurately predict the generated spectra under various conditions. Generally, x-ray prediction models can be divided in three main categories: empirical, semi-empirical and Monte Carlo (MC) calculations [1]. Empirical models are based on the reconstruction of x-ray spectra from experimentally measured transmission data. Semi-empirical models, pioneered by Kramers [2], are based on quantum mechanics theory of bremsstrahlung x-ray production in which the differential cross-section of bremsstrahlung photons is formulated by empirically parameterized differential equations. Whereas, MC simulations which remain the most accurate method are based on random sampling of electron interaction cross sections by which x-ray photons are generated into the target material. The use of MC simulations allows to gain detailed knowledge of x-ray spectra from their outset site in the x-ray tube to the detected spectrum at the image receptor and to separately evaluate the impact of different factors contributing to the generated spectra.

From their emission point in the anode block to the exit window, x-ray photons undergo a tube-specific attenuation pertaining to several absorbing materials, which is collectively referred to as inherent filtration [3]. An initial, sometimes significant inherent filtration takes place within anode material in which depending on tube voltage, anode angle and the roughness of focal path surface x-ray photons are attenuated.

Inherent filtration attenuates low-energy x-rays to a greater extent compared to high energy ones and therefore can contribute effectively to x-ray tube's output. Since x-ray production is an inherently inefficient process, even in targets with high atomic number, less than 1% of the energy deposited in the target appears as x-rays for tubes operated at conventional voltages. Almost all of the energy delivered by impinging electrons is degraded to heat within the target which can rise its temperature up to approximately 2500 C°. This might result in surface roughening and pitting through thermo-mechanical stresses [4]. As reported in the literature, anode roughness act on output spectra as an additional inherent filter which decreases radiation output. Nowotny and Meghzifene determined semi-empirically a variation of about 0.2 mm Al in half value layer (HVL) for an anode roughness of 5 μm at 70 kVp [5]. The same group reported later that anodes with a surface roughness of about 1.4–3.8 μm correspond to additional filtration by tungsten with a thickness of 2.12–8.21 μm [6]. Erdelyi *et al.* presented detailed measurements of anode surface profiles of 19 diagnostic x-ray tubes and predicted semi-empirically an intensity loss of 4% for the most aged anode covered in their work which was roughened by 8 μm-deep cracks [7].

The studied range of roughness reported in the literature is probably not representation of typical situations encountered in the clinic. For instance, Lenz [8] addressed surface roughness of 45 μm for typical x-ray tubes at the end of their lifespan. Moreover, to the authors' knowledge, there has not been any MC study addressing the applicability of empirical and semi-empirical models in treating the issue of anode roughness. The necessity of further investigation motivated us to perform an experimental measurement along with a Monte Carlo-based study using the MCNP4C code.

II. Materials and Methods

A. The MCNP Monte Carlo code

The MCNP code, a general-purpose Monte Carlo radiation transport code [9] was employed to simulate x-ray spectra within x-ray tubes having surface-deteriorated anodes. Over the years, this code has undergone numerous renovations and enhancements through the addition of new features. MCNP has now become one of the most popular and widely used MC codes for neutron, photon and electron transport problems. The rising desire in employing this code returns to its extremely powerful geometry package, detailed physics treatment, various scoring capabilities and extensive internal error-checking routines. MCNP uses a flexible scheme in geometry definition in which geometrical volumes, known as cells, are primarily defined by Boolean combination of first, second and fourth degree surfaces in a three-dimensional Cartesian coordinate system. As an example, a cube can be defined by Boolean intersection of six planes (first degree surfaces). In x-ray generation, it transports electrons into a geometrically-defined tungsten anode based on continuous slowing down approximation (CSDA) energy loss model. According to this model, it breaks electron's path into many steps whose length is derived from total stopping power of the electron in tungsten material. Like most other MC codes, MCNP uses *condensed history* Monte Carlo method for electron transport in which the global effects of electron collisions (energy loss and change of its direction) are sampled at the end of each track segment or step. The energy loss is sampled from Landau distribution by which bremsstrahlung and impact ionization K x-rays are ultimately born into the target medium. The Goudsmit-Saunderson multiple scattering theory is used to sample from the distribution of angular deflections, so that the direction of the electron can change at the end of each track segment. Electrons and their descendents are all tracked to where they are absorbed in or escape from the anode block. MCNP empowers user through several flexible tally treatments especially point-detector tally (F5), a partially-deterministic variance reduction technique by which the flux of generated photons can be scored in the regions appointed at a 100 cm distant point out of x-ray tube.

B. Anode Surface Characterization

Several soon-to-be aged and heavily aged x-ray tubes were gathered and analyzed after cutting out 1 cm × 1 cm pieces from their focal path. For our image-based modeling, a digital image was taken from each anode sample. Fig.1 (a) shows the focal surface of our most aged anode. As can be seen, the surface is so eroded that its cracked and grainy appearance can be observed with the naked eye. The branching pattern of cracks and their invasion into off-focus regions are well depicted in the foreground of this picture. The characterization of focal path surfaces was accomplished by surface profilometry (Taylor Hobson Surtronic, Leicester, UK) and scanning electron microscopy (Leo 440, UK). The roughness profile of our most aged anode indicated that its center-line average roughness (R_a) was about 50 μm and its deepest cracks can grow approximately up to 130 μm deep down into the surface. Fig. 1 (b) shows a 30-times magnified SEM image of that anode sample. As seen, there are regions that have been surrounded by coarser cracks and broken up by finer ones. It was determined that the coarse and fine cracks can have a width of approximately up to 100 and 20 μm, respectively.

C. Rough Surface Models

For more realistic models, the geometry of the anode blocks and their cracked surfaces had to be described into MCNP's environment in as much detail as possible. For this purpose, an image-based modeling method was followed which made it possible to accommodate cracks with their actual pattern into anode models. Basically, our modeling was based on the concept that a continuous rough surface can be approximated by a discrete two-dimensional array of many small cubes having different heights and arranged by a predefined pattern. In this approach, the height and location of each cube can be determined from a per-processed image matrix of focal spot's image. One can imagine as if cubes have been overlaid on the image matrix and each one has received its height from the pixel value of its underlying pixel. To implement this concept onto an MCNP input file, an in-house MATLAB (Math Works Inc., Natick, MA, USA) code was written that defines the cubes in the same number of pixels as exists in the processed matrix and then, raises the height of each cube up to its

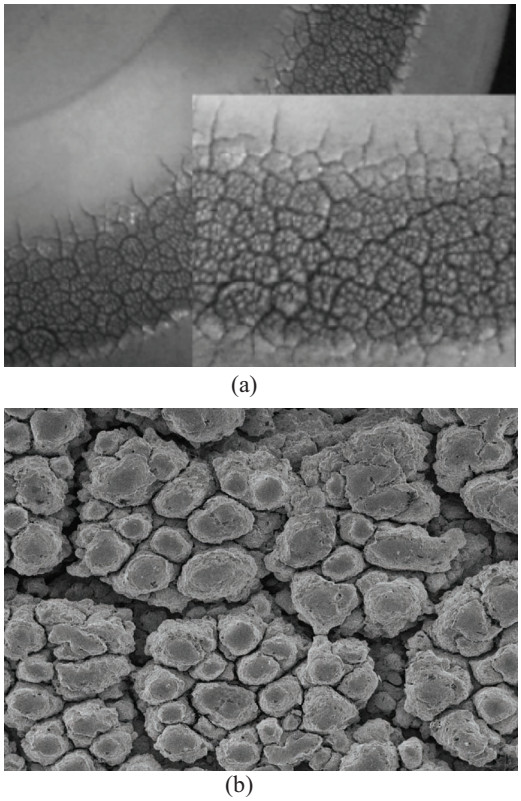

Fig. 1. (a) A digital image taken from the most aged anode disk studied in this work and a close-up from its focal path surface. (b) An SEM image from the central part of the focal path in (a) with a magnification of 30.

predetermined value from its corresponding pixel. Given that centimeter is the unit of length used in MCNP, the image matrices were numerically processed such that the depth of cracks to be incorporated into pixel values agree with the measured average depths. For example, if a cube's height has to be upraised by 5 μm, a value of 5×10^{-4} is allocated to its underlying pixel. Due to the large number of cells and surfaces, a trade-off between the level of models' complexity and MCNP's functionality was admitted. As shown in Fig.2 (a), the roughness of regions bounded by coarse cracks was therefore ignored during the processing of focal spots' image. In addition, the image matrix sizes were shrunk by nearest-neighbor interpolation. Finally, for defining surface models in an optimized way without sacrificing their details, the written code was further developed in such a way that neighboring cells having the same height are merged into a larger cell. As illustrated in Fig. 2 (b), this code combines cells if they share a common boundary, are bounded by the same surfaces in the directions perpendicular to the common boundary, and have the same height. The width and length of each cube were scaled so that the dimensions of the model matched closely those of the actual focal spot. The anode angle is considered in geometry definition by rotating all anode surface planes around an axis to the value of the anode angle. The CAD visualization was translated from MCNP input file of the modeled surface using MCAM software (FDS Team, China, Ref. [10]).

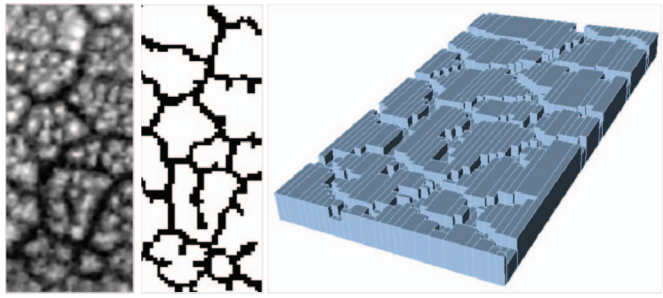

Fig. 2. Illustration of the modeling process for a surface-cracked anode in the 3D coordinate system of MCNP. (a) The digital image of the focal region is processed such that the pattern and the mean depth of main cracks to be rendered into image matrix (according to the surface profilometries, a depth number is assigned to each dark pixel). (b) An optimally defined anode model based on the image in (a) visualized by MCAM.

D. Quantitative assessment strategy

The simulated spectra of surface-cracked anodes were quantitatively assessed through comparison with simulated spectra in a perfectly plain anode under the same conditions of x-ray generation (anode angle, tube voltage, detection point, etc.). The filtering effect of anode roughness reduces both the quality and quantity of the outwardly emitted photons and as such intensity loss was used as a large in scope criterion. The quantification of the overall variations of the spectra was completed using the normalized root mean squared difference (NRMSD), a well-established measure of the difference between estimates predicted by a model and the observed estimates normalized to the range of observed estimates. The heel effect which refers to a falloff in the intensity of radiation field toward the anode side as a result of anode self-filtration was assessed by placing several point detectors (F5) along the anode-cathode direction and keeping them 100 cm away from the focal spot. Finally, change in patient skin entrance dose resulting from anode roughness in chest x-ray radiography examinations was assessed.

E. Validation

The validation of MCNP's output involves comparing simulated and experimentally measured spectra in order to determine whether it faithfully reproduces realistic x-rays spectra. Due to the finite energy resolution of physical detectors, tungsten K-lines of measured spectra appear as broadened peaks. Hence, for the same energy bin, characteristic K x-rays measured by physical detectors always have a lower intensity than those obtained using MC simulations [11]. The shape of a broadened peak can be approximated by a Gaussian function centered at K-line's energy with a width characteristic of the resolution of the employed spectrometer. Detector response was realistically modeled using Gaussian energy broadening (GEB) in which the tallied energies are broadened by sampling from the user-provided Gaussian energy distribution. In our validation, the GEB card was used and its associated parameters experimentally adjusted to fit the full width at half peak maximum (FWHM) of the spectrometer to which simulated spectra were compared.

III. Results

Fig. 3 compares measured and simulated spectra for tube voltages of 125 kVp (anode angle 6˚, total filtration 2.5 mm Al). The spectra measured using a highly pure germanium detector with a FWHM of 0.5 keV at 122 keV (^{57}Co) at the center of the radiation field was obtained from ref. [12]. Both spectra were binned into 1 keV energy intervals and normalized to the sum of all counts. In both simulation runs using 8×10^7 electrons, the GEB card was invoked and provided with appropriate coefficients. As can be seen, the measured and simulated spectra are in very good agreement.

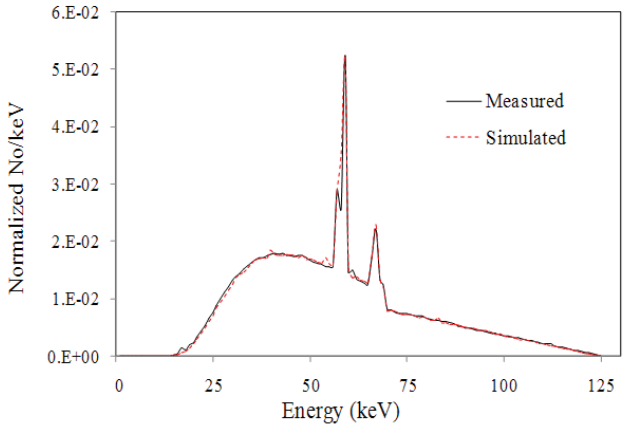

Fig. 3. Comparison of experimental and MCNP4C-simulated x-ray spectra at 125 kVp for a 6° tungsten anode with 2.5 mm Al filtration.

Fig. 4 compares simulated spectra in a plain surface anode and those in rough anodes (5, 10, 20, and 50 μm) at tube voltages of 50, 70, 100 kVps and anode angle of 6 degree. Depending on the depth of cracks both bremsstrahlung and characteristic K x-rays were more attenuated as they experienced further filtration associated with anode roughness. The filtration of emerging x-rays also depends on the anode material, tube voltage and anode angle. As tube voltage increases, the influence of anode roughness is limited to lower energy regions of the spectrum and hence the amount of photon absorption or intensity loss decreases.

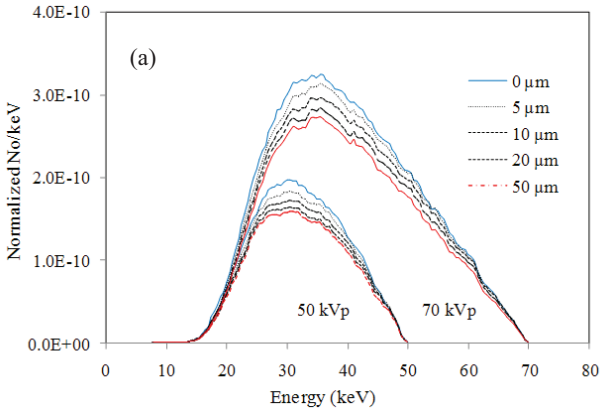

Fig. 4. Comparison of simulated spectra of rough surface anodes with those of plain surface anodes for different crack depths at (a) 50 and 70 kVp (b) 100 kVp (6° tungsten anode with 2.5 mm Al filtration).

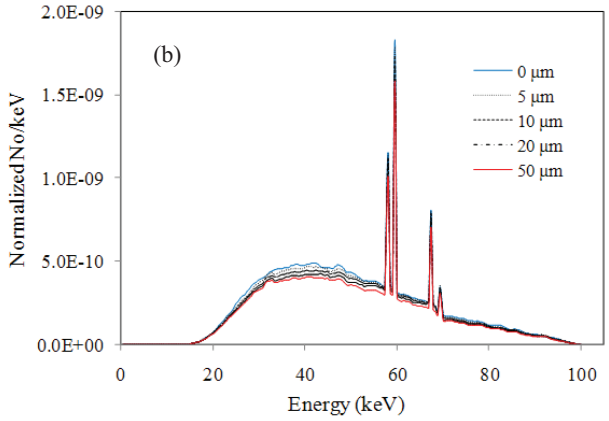

Fig. 4. (Continued).

Table 1 presents the percentage of intensity loss for different crack depths, tube voltages and anode angles calculated by simulating 3.5×10^7 electrons. According to this table, by decreasing tube potential and anode angle and increasing the depth of cracks, the intensity loss becomes more significant (exceeding 16%) at potential of 50 kVp, anode angle of 6° and mean crack depth of 50 μm.

When quantified using the NRMSD, the variations in spectral shape were found to be more pronounced for spectra generated at lower voltages in anodes having deeper cracks and smaller angles.

TABLE I. Percentage of intensity loss for different crack depths, tube voltages and anode angles. The spectra were filtered using 2.5 mm Aluminum and detected at 100 cm from the focal spot.

Anode angle (deg)	Crack depth (μm)	Tube voltage (kVp)				
		50	70	80	100	120
6	5	4.5	3.0	3.1	2.9	2.1
	8	7.7	5.6	5.5	5.0	4.1
	10	9.3	7.1	7.0	6.3	5.3
	15	12.0	9.9	9.3	8.7	7.7
	20	13.6	11.6	11.3	10.4	9.5
	30	15.3	13.8	13.6	12.9	11.9
	50	16.8	15.9	15.7	15.3	14.1
10	5	2.1	1.5	1.4	1.3	1.2
	8	4.4	3.0	2.9	2.8	2.2
	10	5.9	4.0	3.8	3.5	3.0
	15	8.8	6.5	6.3	5.6	5.0
	20	11.0	8.6	8.2	7.4	6.7
	30	13.4	11.2	10.8	9.9	9.2
	50	15.7	14.0	13.6	13.1	12.3
14	5	1.1	1.0	0.7	0.7	0.6
	8	2.4	1.9	1.4	1.5	1.2
	10	3.6	2.5	2.1	2.0	1.6
	15	6.2	4.3	4.0	3.3	3.1
	20	8.7	5.9	5.5	4.7	4.4
	30	11.7	8.7	8.1	7.3	6.8
	50	14.4	11.8	11.4	10.2	9.8

Several point-detector tallies were deployed along anode-cathode direction to evaluate the impact of anode roughening on exposure over the radiation field. It was found that for a 12 degree anode, roughened by 50 μm-deep cracks, the reduction

in exposure is 14.9% and 13.1% for 70 and 120 kVp tube voltages, respectively. Fig. 5 shows this considerable reduction.

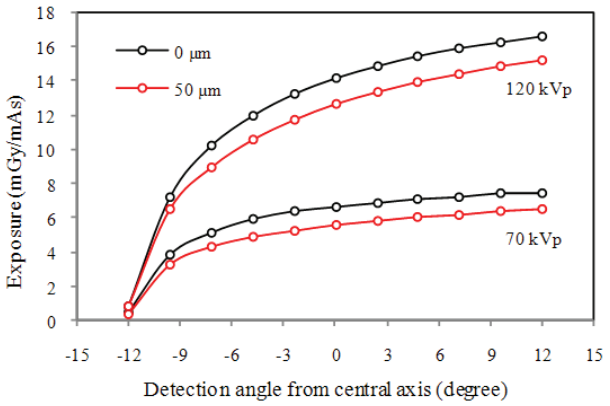

Fig. 5. Effect of anode roughness on the overall reduction of exposure in anode-cathode axis. The spectra were produced in plain and 50 μm deep cracked anodes using 12˚ angle and 70 and 120 kVp tube voltages.

Fig. 6 shows the variation in patient entrance skin dose (ESD) during chest x-ray radiography for an anode angle of 12 degree as a function of crack depth for various tube voltages (between 50 and 140 kVp). The results show that as anode roughness increases, patient entrance skin dose decreases averagely by a factor of 15%. For anode roughness of 50 μm, the ESD decreases by 16.5% and 13.8% at 50 and 140 kVp, respectively.

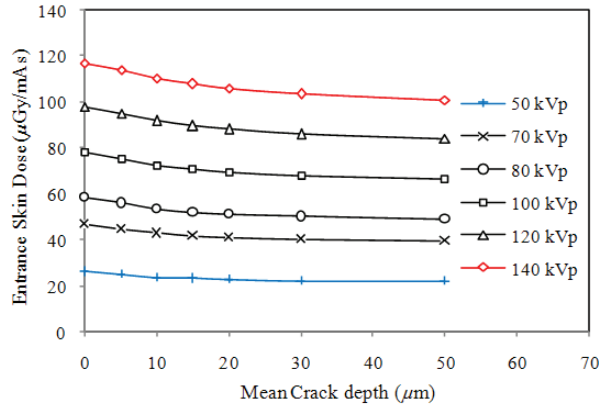

Fig. 5. The variation of patient entrance skin dose (ESD) during x-ray chest radiography for rough-surface anodes having 0 to 50 μm deep cracks. Anode angle is 12 degree and tube potentials vary between 50 and 140 kVp.

IV. Discussion

The prediction of the x-ray spectrum emitted from an x-ray tube can be accurately performed by Monte Carlo simulation. For this purpose, a number of general-purpose MC codes exit. In this work, we used the MCNP code owing to its very powerful geometry package which allows the simulation of an x-ray spectrum in the complex geometry of deteriorated targets. Another motivation behind this choice is our previous experience with this code for similar purposes. As shown in Fig. 3, comparisons with experimental spectra proved that in equal conditions, by calling its GEB card, MCNP can faithfully predict x-ray spectra. The minor mismatch occurred in the region between tungsten $K\alpha_1$ and $K\alpha_2$ peaks, in which MCNP point detector could not resolve peaks as good as the physical detector. This can also be explained by the fact that the detector response is approximated by a Gaussian function whose coefficients may not be perfectly adjusted. It is worth to note that by running 8×10^7 electrons and making use of point-detector tally, a partially-deterministic variance reduction technique, the relative error of photon flux was minimized to 0.21%.

By means of Monte Carlo simulations, it has been shown that highly accelerated electrons in conventional x-ray tubes can penetrate into the tungsten target up to 14 μm [13]. When such electrons fall into the anode's cracks, they can penetrate more and as such the associated x-rays which were previously shallowly produced must go through a longer attenuating path before reaching the surface. Moreover, these x-rays may end up in the cracks and then be scattered by a few interactions with their walls. Thus, it can be said that the decreased output radiation brought about by anode roughness results from the increased anode self-filtration as well as the excessive scattering of x-rays toward directions away from the exit window.

In agreement with the work of Erdelyi *et al* [7], our results showed that a 5% intensity loss for anodes aged by 8 μm deep cracks (anode angle of 6°, tube potential of 100 kVp). Lenz [8] claimed that long-term tests have been shown that anode roughness at the end of a typical tube's lifespan can be 45 μm which can cause a weakening of output radiation by 14% or even more. In our work, the output reduction (μGy/mAs) for an anode roughness of 50 μm at tube voltage of 80 kVp (as the mean voltage between 50 and 120 kVp) and in anode angle of 10 degrees (as the mean angle between 6 and 14 degrees) was found to be 14.7% which is in close agreement with Lenz's results.

Fig. 5 indicated that anode roughening has a considerable effect on exposure rate in the radiation field and consequently, as Fig. 6 shows, impacts patient dose.

V. Conclusion

By employing MCNP4C code and defining more realistic models from surface-deteriorated anodes into its environment, it was attempted to evaluate how effectively anode surface roughness can affect diagnostic x-ray spectra. SEM measurements showed a significant grain growth and crack formation in our most aged anode. Surface profilometry highlighted that center-line average roughness (R_a) can go up to 50 μm. It was predicted that an intensity loss of 4.5% and 16.8% might result from anodes aged by 5 and 50 μm-deep cracks under the conditions of 50 kVp, 6˚ target angle and 2.5 mm Al total filtration. We conclude that anode roughening can have not only a non negligible but in some cases a considerable effect on output spectra and should be considered when x-ray imaging tubes become old and overworked.

References

[1] M. R. Ay and H. Zaidi, "Analytical and Monte Carlo X-ray Spectra Modeling in Mammography," in *Emerging Technology in Breast Imaging and Mammography*, J. Suri, R. M. Rangayyan, and S. Laxminarayan, Eds.: American Scientific, 2007.

[2] H. A. Kramers, "On the theory of x-ray absorption and of the continuous x-ray spectrum," *Philos Mag,* vol. 46, pp. 836-871, 1923.
[3] W. R. Hendee and E. R. Ritenour, *Medical Imaging Physics*, 4th ed.: Wiley-Liss, Inc., 2002.
[4] J. T. Bushberg, J. A. Setbert, E. M. Letdholdt, and J. M. Boon, *The Essential Physics Of Medical Imaging*, 2th ed.: Lippincott Williams & Wilkins, 2002.
[5] R. Nowotny and K. Meghzifene, "Simulation of the effect of anode surface roughness on diagnostic x-ray spectra," *Phys Med Biol,* vol. 47, pp. 3973-83, Nov 21 2002.
[6] K. Meghzifene, H. Aiginger, and R. Nowotny, "A fit method for the determination of inherent filtration with diagnostic x-ray units," *Phys Med Biol,* vol. 51, pp. 2585-97, May 21 2006.
[7] M. Erdelyi, M. Lajko, R. Kakonyi, and G. Szabo, "Measurement of the x-ray tube anodes' surface profile and its effects on the x-ray spectra," *Med Phys,* vol. 36, pp. 587-93, Feb 2009.
[8] E. Lenz, "X-ray anode having an electron incident surface scored by microslits," in *Siemens Aktiengesellschaft* Munich DE, 2006.
[9] J. F. Briesmeister, "MCNP—A general Monte Carlo N-particle transport code," Los Alamos National Laboratory LA-13709-M, 2000.
[10] Y. Wu, "CAD-based interface programs for fusion neutron transport simulation," *Fusion Eng. Des.,* vol. 84, pp. 1987-1992, 2009.
[11] M. Bazalova and F. Verhaegen, "Monte Carlo simulation of a computed tomography x-ray tube," *Phys Med Biol,* vol. 52, pp. 5945-55, Oct 7 2007.
[12] H. Aichinger, J. Dierker, S. Joite-BarfuB, and M. Sabel, *Radiation exposure and image quality in x-ray diagnostic radiology, Physical principles and clinical applications*, 1th ed. Berlin Heidelberg: Springer, 2004.
[13] G. G. Poludniowski and P. M. Evans, "Calculation of x-ray spectra emerging from an x-ray tube. Part I. electron penetration characteristics in x-ray targets," *Med Phys,* vol. 34, pp. 2164-74, Jun 2007.